

Old Dominion University
ODU Digital Commons

Physics Faculty Publications

Physics

2003

Final State Interaction Effects in ^3He ($e \rightarrow, e' p$)

C. Carasco

J. Bermuth


P. Merle

P. Bartsch

D. Baumann

See next page for additional authors

Follow this and additional works at: https://digitalcommons.odu.edu/physics_fac_pubs

 Part of the [Astrophysics and Astronomy Commons](#), [Elementary Particles and Fields and String Theory Commons](#), and the [Nuclear Commons](#)

Original Publication Citation

Carasco, C., Bermuth, J., Merle, P., Bartsch, P., Baumann, D., Bohm, R., . . . Zeier, M. (2003). Final state interaction effects in $^3\text{He}(e \rightarrow, e' p)$. *Physics Letters B*, 559(1-2), 41-48. doi:10.1016/S0370-2693(03)00306-x

This Article is brought to you for free and open access by the Physics at ODU Digital Commons. It has been accepted for inclusion in Physics Faculty Publications by an authorized administrator of ODU Digital Commons. For more information, please contact digitalcommons@odu.edu.

Authors

C. Carasco, J. Bermuth, P. Merle, P. Bartsch, D. Baumann, R. Böhm, D. Bosnar, M. Ding, M. O. Distler, and A. Klein



ELSEVIER

Available online at www.sciencedirect.com

SCIENCE @ DIRECT®

PHYSICS LETTERS B

Physics Letters B 559 (2003) 41–48

www.elsevier.com/locate/npe

Final state interaction effects in ${}^3\overline{\text{He}}(\vec{e}, e'p)$

C. Carasco^a, J. Bermuth^g, P. Merle^f, P. Bartsch^f, D. Baumann^f, R. Böhm^f,
D. Bosnar^k, M. Ding^f, M.O. Distler^f, J. Friedrich^f, J.M. Friedrich^f, J. Golak^d,
W. Glöckle^b, M. Hauger^a, W. Heil^g, P. Jennewein^f, J. Jourdan^{a,*}, H. Kamadaⁱ,
A. Klein^h, M. Kohl^c, K.W. Krygier^f, H. Merkel^f, U. Müller^f, R. Neuhausen^f,
A. Nogga^j, Ch. Normand^a, E. Otten^g, Th. Pospischil^f, M. Potokar^e, D. Rohe^a,
H. Schmieden^f, J. Schmiedeskamp^g, M. Seimetz^f, I. Sick^a, S. Širca^e, R. Skibiński^d,
G. Testa^a, Th. Walcher^f, G. Warren^a, M. Weis^f, H. Witała^d, H. Wöhrle^a, M. Zeier^a

^a Department für Physik und Astronomie, Universität Basel, Switzerland

^b Institut für Theoretische Physik II, Ruhr-Universität Bochum, Germany

^c Institut für Kernphysik, Technische Universität Darmstadt, Germany

^d Institute of Physics, Jagiellonian University, Kraków, Poland

^e Institute Jožef Stefan, University of Ljubljana, Ljubljana, Slovenia

^f Institut für Kernphysik, Johannes Gutenberg-Universität, Mainz, Germany

^g Institut für Physik, Johannes Gutenberg-Universität, Mainz, Germany

^h Department of Physics, Old Dominion University, Norfolk, USA

ⁱ Department of Physics, Kyushu Institute of Technology, Tobata, Kitakyushu, Japan

^j Department of Physics, University of Arizona, Tucson, AZ, USA

^k Department of Physics, University of Zagreb, Croatia

Received 27 January 2003; received in revised form 26 February 2003; accepted 26 February 2003

Editor: J.P. Schiffer

Abstract

Asymmetries in quasi-elastic ${}^3\overline{\text{He}}(\vec{e}, e'p)$ have been measured at a momentum transfer of $0.67 \text{ (GeV}/c)^2$ and are compared to a calculation which takes into account relativistic kinematics in the final state and a relativistic one-body current operator. With an exact solution of the Faddeev equation for the ${}^3\text{He}$ -ground state and an approximate treatment of final state interactions in the continuum good agreement is found with the experimental data.

© 2003 Published by Elsevier Science B.V. Open access under [CC BY license](https://creativecommons.org/licenses/by/4.0/).

PACS: 21.45.+v; 25.10.+s; 24.70.+s; 25.30.Fj

Keywords: Polarized electron scattering; ${}^3\text{He}$ -structure; Final-state interaction

* Corresponding author.

E-mail address: juerg.jourdan@unibas.ch (J. Jourdan).

Introduction

Investigations of the structure of the nuclear three-body system have recently attracted much interest. Modern three-body calculations allow for a quantitative description of this system not only of the ground state but also for the continuum states. Results of such calculations open the possibility to test our understanding of the three-body system, the role of three-body forces, and non-nucleonic degrees of freedom by using continuum observables, quantities that obviously have a much richer structure and contain additional information. These calculations have reached a high degree of sophistication, and several “exact” calculations are available today [1,2].

Recently, ${}^3\text{He}$ became also important for studies of nucleon form factors. Due to the lack of free neutron targets, only neutrons bound in light nuclei can be studied. The main advantage of ${}^3\text{He}$ lies in the fact that for the major part of the ground state wave function the spins of the two protons are antiparallel so that spin-dependent observables are dominated by the neutron [3].

When using ${}^3\text{He}$ as a neutron target, nuclear structure effects such as final state interactions (FSI), meson exchange currents (MEC), and relativistic effects must be carefully considered [4]. With the calculations available today such corrections can be performed quantitatively at low Q^2 as was demonstrated in the recent electromagnetic form factor experiments by Becker et al. and Xu et al. [5,6]. However, given that the calculations were performed in a non-relativistic framework, a “rigorous” treatment of these corrections at higher Q^2 was not at hand. This represents a serious difficulty for experiments aiming at the electric neutron form factor, G_{en} .

The present Letter reports about a new, less rigorous approach to correct for nuclear effects at high Q^2 . The theoretical results are compared with asymmetries measured in quasi-elastic ${}^3\text{He}(\vec{e}, e'p)$ -scattering at $Q^2 = 0.67 \text{ (GeV}/c)^2$.

Theory

The calculation is based on an exact, but non-relativistic ${}^3\text{He}$ ground state wave function. To obtain the matrix elements relativistic kinematics and a relativistic single nucleon current operator are used. Thereby the final state includes rescattering terms to first order in the nucleon–nucleon (NN) t-matrix. Results for the AV18 NN-potential [7] will be presented. The dependence on the NN-interaction is studied with a calculation which employs the CD–Bonn NN-potential [8]. In order to provide insight into the importance of relativity additional calculations with a non-relativistic current or with non-relativistic kinematics are performed. All calculations use the parameterization by Höhler to describe the electromagnetic form factors of the nucleons [9].

As mentioned above, ${}^3\text{He}(\vec{e}, e'N)$ at large Q^2 does not allow for a rigorous treatment of FSI based on the Faddeev-like integral equation [1]. When the center-of-mass energy of the three-nucleon (3N) system is well above the pion production threshold the usual potential approach is not valid. However, in quasi-elastic kinematics the focus is mostly on the region of phase space, where one of the nucleons is struck with a high energy and momentum and leaves the remaining two-nucleon system with a rather small internal energy. Thus, one may hope that approximations shown in Fig. 1 will be justified.

Let us first consider the three-body breakup of ${}^3\text{He}$. The amplitude A_1 takes a very simple form

$$A_1 = \langle \vec{p}_1 m_1 v_1 \vec{p}_2 m_2 v_2 \vec{p}_3 m_3 v_3 | j(\vec{Q}, 1) | \Psi_b \vec{P} M M_T \rangle, \quad (1)$$

where \vec{p}_i are the individual nucleon momenta and m_i (v_i) their spin (isospin) projections. \vec{P} is the total momentum and M (M_T) the spin (isospin) magnetic quantum number of the initial ${}^3\text{He}$ bound state. The single nucleon current $j(\vec{Q}, 1)$ acts only on nucleon 1. Choosing the laboratory frame $\vec{P} = 0$ and the standard representation of the 3N bound state in the basis of relative Jacobi momenta \vec{p} and \vec{q} one gets

$$A_1 = \delta(\vec{p}_1 + \vec{p}_2 + \vec{p}_3 - \vec{Q}) \sum_{m'_1} j(\vec{p}_1, \vec{p}_1 - \vec{Q}; m_1, m'_1; v_1) \langle \vec{p} \vec{q} m'_1 m_2 m_3 v_1 v_2 v_3 | \Psi_b M M_T \rangle, \quad (2)$$

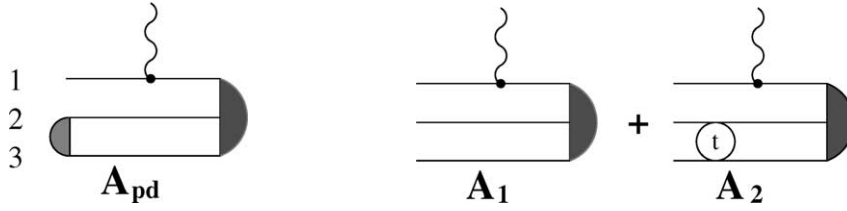


Fig. 1. Diagrammatic representation of the two-body (left) and three-body (right) breakup of ${}^3\text{He}$. The curly lines denote the photon coupling to nucleon 1. The large (small) semi-circles depict the ${}^3\text{He}$ (deuteron) bound state. In A_1 FSI is neglected, in A_2 the scattering operator t acts only in the subsystem (23). Note, that for the two-body breakup there is no diagram corresponding to A_2 .

where $\vec{p} = \frac{1}{2}(\vec{p}_2 - \vec{p}_3)$, $\vec{q} = \vec{p}_1 - \vec{Q}$. Finally, we use the partial wave decomposition of the bound state in the basis $|pq\alpha\rangle$ (see [10]) and arrive at

$$\begin{aligned}
 A_1 &= \delta(\vec{p}_1 + \vec{p}_2 + \vec{p}_3 - \vec{Q}) \delta_{v_1+v_2+v_3, M_T} \sum_{m'_1} j(\vec{p}_1, \vec{p}_1 - \vec{Q}; m_1, m'_1; v_1) \\
 &\times \sum_{\alpha'} \sum_{\mu'} C(j', I', \frac{1}{2}; \mu', M - \mu', M) C(l', s', j'; \mu' - m_2 - m_3, m_2 + m_3, \mu') \\
 &\times C(\frac{1}{2}, \frac{1}{2}, s'; m_2, m_3, m_2 + m_3) C(\lambda', \frac{1}{2}, I'; M - \mu' - m'_1, m'_1, M - \mu') \\
 &\times C(t', \frac{1}{2}, \frac{1}{2}; v_2 + v_3, v_1, v_1 + v_2 + v_3) C(\frac{1}{2}, \frac{1}{2}, t'; v_2, v_3, v_2 + v_3) \\
 &\times Y_{l', \mu' - m_2 - m_3}(\hat{p}) Y_{\lambda', M - \mu' - m'_1}(\hat{q}) \langle pq\alpha' | \Psi_b \rangle. \tag{3}
 \end{aligned}$$

The amplitude A_2 is given by

$$A_2 = \langle \vec{p}_1 m_1 v_1 \vec{p}_2 m_2 v_2 \vec{p}_3 m_3 v_3 | t_{23} G_0 j(\vec{Q}, 1) | \Psi_b \vec{P} M M_T \rangle \tag{4}$$

and can be written as

$$\begin{aligned}
 A_2 &= \delta(\vec{p}_1 + \vec{p}_2 + \vec{p}_3 - \vec{Q}) \delta_{v_1+v_2+v_3, M_T} \delta_{v_1, v'_1} \sum_{m'_1} j(\vec{p}_1, \vec{p}_1 - \vec{Q}; m_1, m'_1; v_1) \\
 &\times \int d\vec{p}' \sum_{m'_2, m'_3} \sum_{v'_2, v'_3} \delta_{v_2+v_3, v'_2+v'_3} \langle \vec{p} m_2 m_3 v_2 v_3 | t(z) | \vec{p}' m'_2 m'_3 v'_2 v'_3 \rangle \\
 &\times \frac{1}{E - E(p_1, p_{23}, p') + i\epsilon} \langle \vec{p}' \vec{q} m'_1 m'_2 m'_3 v'_1 v'_2 v'_3 | \Psi_b M M_T \rangle, \tag{5}
 \end{aligned}$$

where $\vec{q} = \vec{p}_1 - \vec{Q}$ and $\vec{p}_{23} = \vec{p}_2 + \vec{p}_3$. The total energy E of the 3N system can be expressed as

$$\begin{aligned}
 E &= \omega + m_{3\text{He}} = \sqrt{m_N^2 + p_1^2} + \sqrt{4(m_N^2 + p^2) + p_{23}^2} \\
 &\approx \sqrt{m_N^2 + p_1^2} + \sqrt{4m_N^2 + p_{23}^2} + \frac{p^2}{\sqrt{m_N^2 + \frac{1}{4}p_{23}^2}} \equiv E(p_1, p_{23}, p), \tag{6}
 \end{aligned}$$

with m_N the nucleon mass. In Eq. (6) \vec{p} is the (relativistic) relative momentum between nucleons 2 and 3 calculated in the frame where the total momentum of the (23) pair is zero. It agrees, however, to a good approximation with the standard (nonrelativistic) definition $\vec{p} = \frac{1}{2}(\vec{p}_2 - \vec{p}_3)$. Consequently, the (23) subsystem internal energy which enters in the nonrelativistic t-matrix calculation is taken as

$$z = E - \sqrt{m_N^2 + p_1^2} - \sqrt{4m_N^2 + p_{23}^2}. \tag{7}$$

In a final step both the bound state wave function and the t-matrix are given in the partial wave basis, which yields

$$\begin{aligned}
A_2 = & \delta(\vec{p}_1 + \vec{p}_2 + \vec{p}_3 - \vec{Q}) \delta_{\nu_1 + \nu_2 + \nu_3, M_T} \sum_{m'_1} j(\vec{p}_1, \vec{p}_1 - \vec{Q}; m_1, m'_1; \nu_1) \\
& \times \sum_{lsj\mu t} C(l, s, j; \mu - m_2 - m_3, m_2 + m_3, \mu) C\left(\frac{1}{2}, \frac{1}{2}, s; m_2, m_3, m_2 + m_3\right) \\
& \times C\left(t, \frac{1}{2}, \frac{1}{2}; \nu_2 + \nu_3, \nu_1, \nu_1 + \nu_2 + \nu_3\right) C\left(\frac{1}{2}, \frac{1}{2}, t; \nu_2, \nu_3, \nu_2 + \nu_3\right) Y_{l, \mu - m_2 - m_3}(\hat{p}) \\
& \times \sum_{\bar{l}} \sum_{\alpha'} \delta_{l\bar{l}} \delta_{s's} \delta_{j'j} \delta_{t't} C(j, I', \frac{1}{2}; \mu, M - \mu, M) C(\lambda', \frac{1}{2}, I'; M - \mu - m'_1, m'_1, M - \mu) \\
& \times Y_{\lambda', M - \mu - m'_1}(\hat{q}) \int dp' (p')^2 \frac{\langle p' q \alpha' | \Psi_b \rangle}{E - E(p_1, p_{23}, p') + i\epsilon} \langle p(ls)jt | t(z) | p'(l's')jt \rangle. \tag{8}
\end{aligned}$$

The amplitude for the two-body breakup of ${}^3\text{He}$, A_{pd} , is given as

$$A_{\text{pd}} = \langle \vec{p}_1 m_1 \nu_1 \phi_d \vec{p}_d m_d | j(\vec{Q}, 1) | \Psi_b \vec{P} M M_T \rangle, \tag{9}$$

where ϕ_d is the deuteron state with the spin magnetic quantum number m_d and laboratory momentum \vec{p}_d . In the next step one gets

$$A_{\text{pd}} = \delta(\vec{p}_1 + \vec{p}_d - \vec{Q}) \delta_{\nu_1 M_T} \sum_{m'_1} j(\vec{p}_1, \vec{p}_1 - \vec{Q}; m_1, m'_1; \nu_1) \langle \vec{q} m'_1 \nu_1 \phi_d \vec{p}_d m_d | \Psi_b M M_T \rangle, \tag{10}$$

where $\vec{q} = \vec{p}_1 - \vec{Q}$. Partial wave expansion of the deuteron and ${}^3\text{He}$ bound state leads to

$$\begin{aligned}
A_{\text{pd}} = & \delta(\vec{p}_1 + \vec{p}_d - \vec{Q}) \delta_{\nu_1 M_T} \sum_{m'_1} j(\vec{p}_1, \vec{p}_1 - \vec{Q}; m_1, m'_1; \nu_1) \\
& \times \sum_{\alpha'} (\delta_{l'0} + \delta_{l'2}) \delta_{s's'} \delta_{j'j} \delta_{t't} C(j', I', \frac{1}{2}; m_d, M - m_d, M) C(\lambda', \frac{1}{2}, I'; M - m_d - m'_1, m'_1, M - m_d) \\
& \times Y_{\lambda', M - m_d - m'_1}(\hat{q}) \int dp' (p')^2 \varphi_{l'}(p') \langle p' q \alpha' | \Psi_b \rangle. \tag{11}
\end{aligned}$$

The single nucleon current matrix elements $j(\vec{p}_1, \vec{p}'_1; m_1, m'_1; \nu_1)$ (ν_1 decides whether the photon couples to the proton or to the deuteron) are taken completely relativistically, i.e.,

$$\begin{aligned}
j(\vec{p}_1, \vec{p}'_1; m_1, m'_1) & \equiv j^\mu(\vec{p}_1, \vec{p}'_1; m_1, m'_1) \\
& = \sqrt{\frac{m_N}{\sqrt{m_N^2 + p^2}}} \sqrt{\frac{m_N}{\sqrt{m_N^2 + p'^2}}} \bar{u}(p m_1) (F_1 \gamma^\mu + i F_2 \sigma^{\mu\nu} (p - p')_\nu) u(p' m'_1). \tag{12}
\end{aligned}$$

In the case of A_{pd} only the proton single nucleon current contributes ($\nu_1 = M_T = \frac{1}{2}$). The amplitudes A_1 , A_2 and A_{pd} are used to calculate the response functions entering the cross sections and the polarization observables.

To simplify integrations over the unobserved parameters of the final 3N system we change the variables according to [11]:

$$d^3 p_1 d^3 p_2 d^3 p_3 = \mathcal{I} d^3 p_1 d^3 p_{23} d^3 p \quad \text{with} \quad \mathcal{I} = \frac{4E_2 E_3}{(E_2 + E_3) \sqrt{(E_2 + E_3)^2 - p_{23}^2}} \tag{13}$$

(E_i is the total energy of the i th nucleon).

Experiment

Asymmetries of the ${}^3\vec{\text{He}}(\vec{e}, e'p)$ -reaction have been measured in quasi-elastic kinematics at a four momentum transfer of $Q^2 = 0.67 \text{ (GeV}/c)^2$. As the spin asymmetry of protons in ${}^3\text{He}$ is very small [4] one can expect that the asymmetries of the ${}^3\vec{\text{He}}(\vec{e}, e'p)$ reaction are very sensitive to FSI and provide a significant test of the calculations.

For an arbitrary direction of the target spin the asymmetry is given by

$$A(\theta^*, \phi^*) = \frac{1}{P_e P_t} \frac{N^+ - N^-}{N^+ + N^-} \quad (14)$$

with θ^* , ϕ^* the polar and azimuthal angle of the target spin direction with respect to the three-momentum transfer \vec{q} . The polarizations of beam and target are given by P_e and P_t and the normalized ${}^3\vec{\text{He}}(\vec{e}, e'p)$ events for positive (negative) electron helicity are N^+ (N^-). The two asymmetries A_{\parallel} and A_{\perp} measured in the present work are $A_{\perp} = A(90^\circ, 0^\circ)$ and $A_{\parallel} = A(0^\circ, 0^\circ)$ [12].

The setup of the experiment was very similar to the one described by Rohe et al. [13]. A polarized continuous wave electron beam with an energy of 854.5 MeV was incident on a glass cell filled with polarized ${}^3\text{He}$. Longitudinally polarized electrons of $\sim 80\%$ polarization were produced with a strained layer GaAsP crystal at a typical current of 10 μA [14]. Spectrometer A with a solid angle of 28 msr and a momentum acceptance of 20% [15] was used to detect the scattered electron at a scattering angle of 78.6° . The struck protons were detected in coincidence with an array of plastic scintillator bars placed at 32.2° , the direction of \vec{q} for an energy transfer ω of 368 MeV.

The ${}^3\vec{\text{He}}$ -target consisted of a spherical glass container with two cylindrical extensions. The beam enters and exits through 25 μm Cu-windows. The cylindrical extensions allowed for an effective shielding of the background from the Cu-windows by positioning the windows outside of the acceptance of the spectrometer. The ${}^3\text{He}$ gas was polarized by metastable optical pumping at pressures around 1 mbar and subsequently compressed by a two-stage titanium piston compressor to 4 bar. The target polarization achieved was approximately 50% [16].

The entire target was enclosed in a rectangular box of 2 mm thick μ -metal and iron. The box served as an effective shield for the stray field of the magnetic spectrometers and provided a homogeneous magnetic guiding field of $\approx 4 \times 10^{-4}$ T produced by three independent pairs of coils. With additional correction coils a relative field gradient of less than $5 \times 10^{-4} \text{ cm}^{-1}$ was achieved. The setup allowed for an independent rotation of the target spin in any desired direction by remote control. In order to reduce systematic errors, the spin of the target was circularly rotated in the scattering plane by 90° with respect to the direction of \vec{q} at regular intervals, alternatively accumulating data for A_{\parallel} and A_{\perp} .

The hadron detector consists of an array of four layers of five vertically placed plastic scintillator bars with dimensions $50 \times 10 \times 10 \text{ cm}^3$ preceded by two layers of 1 cm thick ΔE detectors for particle identification. Every plastic bar was equipped with two Photo Multipliers (PM) on top and bottom. The detector was placed at 32.2° at a distance of 160 cm from the target which resulted in a solid angle of 100 msr. The entire detector was shielded with 10 cm Pb except for an opening towards the target where the Pb-shield was reduced to 2 cm.

As in the experiment by Rohe et al. [13] the product of target and beam polarization was monitored during the data taking via determination of the asymmetry for elastic ${}^3\vec{\text{He}}(\vec{e}, e)$ -scattering. The ${}^3\text{He}$ -form factors are accurately known [17] and the comparison of the calculated and measured asymmetry allows for a precise determination of the polarization product $P_e P_t$. The elastically scattered electrons were detected in spectrometer B at a scattering angle of $\vartheta_e = 25^\circ$. This resulted in a polarization product of 0.279 ± 0.010 for runs with $A = A_{\parallel}$ or $-A_{\parallel}$ and 0.282 ± 0.003 for $A = A_{\perp}$ or $-A_{\perp}$. The difference of the error bar results from the different sensitivity of the measurement to the target spin direction.

In addition, the time dependence of the polarization of the target cell was continuously measured during the experiment by Nuclear Magnetic Resonance, while the absolute polarization was measured by the method of Adiabatic Fast Passage [18]. The mean target polarization from these measurements was 0.356 ± 0.015 . From

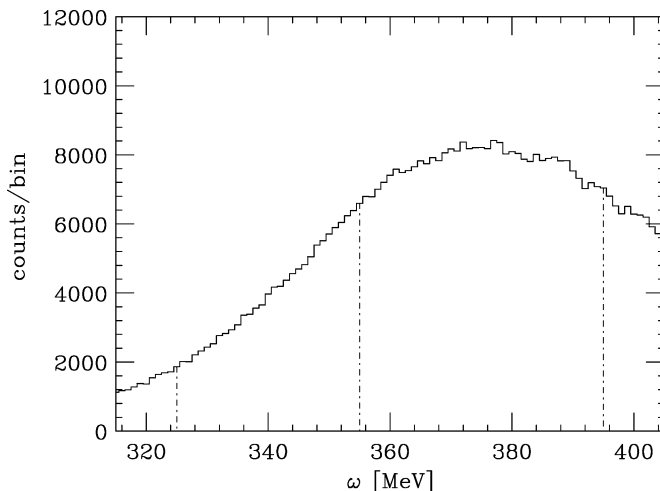


Fig. 2. Experimental spectrum of the ${}^3\text{He}(\vec{e}, e'p)$ -data as a function of the energy transfer ω . The dot-dashed lines indicate the two regions selected for the analysis.

the elastic scattering data and the target polarization measurements a beam polarization of $P_e = 0.788 \pm 0.036$ was determined which agreed well with the result from a Møller polarimeter (0.827 ± 0.017).

Analysis

In the off-line analysis, protons are defined as events with a hit in two consecutive ΔE detectors from the two ΔE -detector planes. For the kinematics of the experiment the proton energies range from ~ 280 MeV to ~ 400 MeV. For this energy range protons reach at least the third bar layer. A correct mean time of at least three plastic bars is also required. For the combination of these cuts negligible background survives in the ${}^3\text{He}(\vec{e}, e'p)$ coincidence time peak. The segmentation of the hadron detector and the up-down PM readout allow for the determination of the direction of the protons. The resolution is $\sim 0.8^\circ$ in both vertical and horizontal direction.

In order to study the effect of FSI on the asymmetries in different kinematic regions, the quasi-elastic peak is divided in two regions of ω . One region covers the peak and therefore emphasizes low nucleon momenta whereas the other region covers the low ω tail sensitive preferentially to high nucleon momenta. Fig. 2 shows the ω spectrum of ${}^3\text{He}(\vec{e}, e'p)$ -events and indicates the two kinematic regions. The events in each of the two regions are summed over the entire acceptance of the out-of-plane angle of electron and proton and over the electron scattering angle in a range from 75.8° to 81.8° .

Results

The experimental results for A_{\parallel} and A_{\perp} are shown in Figs. 3 and 4 compared to the results of the plane wave impulse approximation (PWIA) and the calculation including the dominant FSI effect. As expected the asymmetries are small over the entire kinematic region so that FSI effects appear prominently. Compared to the statistical accuracy (0.02–0.03) the systematic errors are small (0.01). The error of the deviation of \vec{q} from its nominal direction, which is usually the dominant systematic error in electric form factor determinations [13], is negligible here mainly because A_{\parallel} and A_{\perp} are not very different from each other.

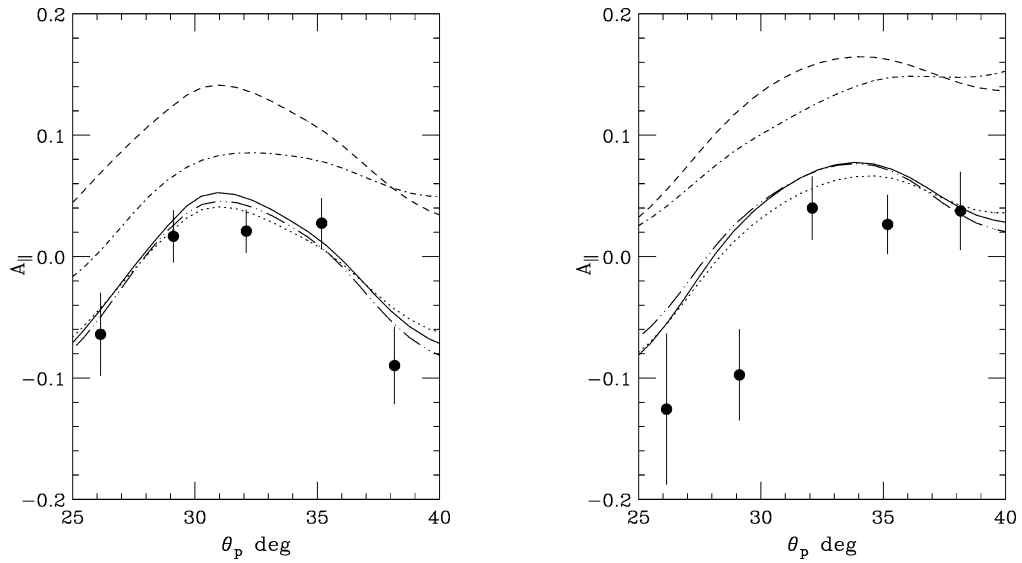


Fig. 3. Experimental results of A_{\parallel} for the quasi-elastic peak region (left) and the low ω tail region (right) as a function of the scattering angle of the knocked out proton. The results of the full (PWIA) calculation are shown with solid (dashed) lines. The result of the full calculation with a non-relativistic current (dot), the effect of a $(v/c)^2$ correction (dot-dot-dash) and the same with non-relativistic kinematics (dot-dash) are also shown.

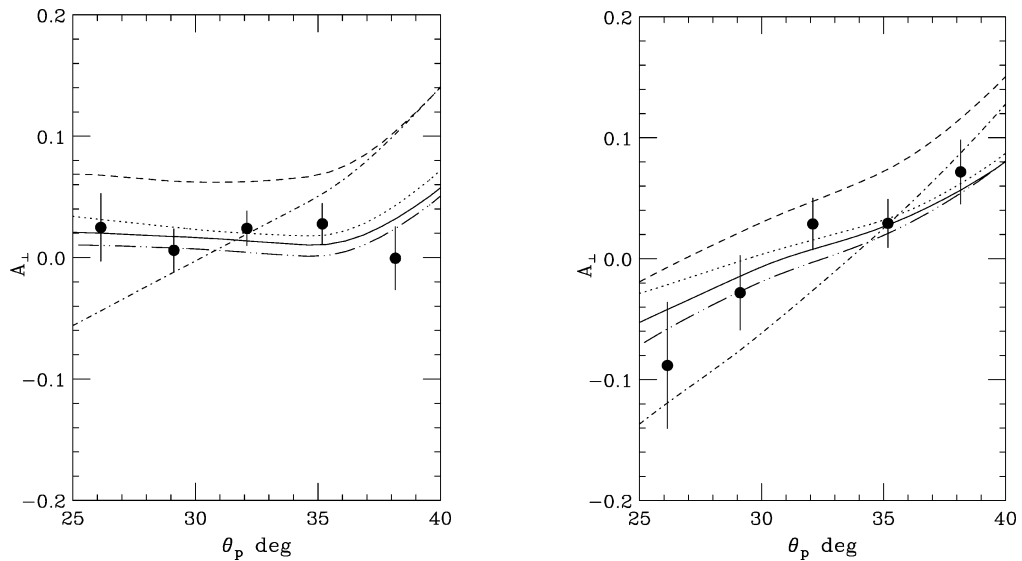


Fig. 4. Same as Fig. 3, but for A_{\perp} .

The hadron detector does not allow for a high-resolution determination of the proton energy. In particular, it is not possible to distinguish two- and three-body breakup events. Accordingly, the calculations have been integrated over the two-body and over the first 26 MeV of the three-body breakup channel. For the highest accepted missing energy of 26 MeV, the cross section is smaller by at least one order of magnitude compared to the cross section

at threshold. Extending the integration limit has no effect on the results. In addition, the calculated results are integrated over the experimentally accepted out-of-plane proton angle and the relevant ω range (Fig. 2).

Conclusions

Figs. 3 and 4 show that the PWIA calculations are in clear disagreement with the experimental results. The same holds for the calculation which does not account for relativistic kinematics. On the other hand, very good agreement between experiment and theory is found when including the A_2 -term of Fig. 1 and accounting for relativistic kinematics. This applies also for the results using the CD–Bonn NN-potential with negligible differences. Small differences of the results are observed when the current is replaced by a non-relativistic version or when a relativistic $(v/c)^2$ -correction is added. The results indicate that at high Q^2 , where complete non-relativistic calculations are not applicable anymore, a good description of the data can be achieved taking into account relativistic kinematics and an approximate treatment of FSI-effects. The use of a relativistic current operator is less relevant. The result is important for experiments aimed at extracting fundamental properties of the neutron from asymmetry measurements of inclusive ${}^3\text{He}(\vec{e}, e')$ or exclusive ${}^3\text{He}(\vec{e}, e'n)$ reactions. The corrections for FSI-effects for these reactions can be reliably calculated within the approach presented here.

Acknowledgements

This work was supported by the Schweizerische Nationalfonds, Deutsche Forschungsgemeinschaft (SFB 443), the Polish Committee for Scientific Research, the Foundation for Polish Science and NSF grant #PHY 0070858. The numerical calculations have been performed on the Cray SV1 of the NIC, Jülich, Germany.

References

- [1] W. Glöckle, et al., Phys. Rep. 274 (1996) 107.
- [2] H. Witała, et al., Phys. Rev. C 63 (2001) 024003.
- [3] J. Golak, et al., Phys. Rev. C 65 (2002) 044002.
- [4] R.W. Schulze, P.U. Sauer, Phys. Rev. C 48 (1993) 38.
- [5] J. Becker, et al., Eur. Phys. J. A 6 (1999) 329;
J. Golak, et al., Phys. Rev. C 63 (2001) 034006.
- [6] W. Xu, et al., Phys. Rev. Lett. 85 (2000) 2900.
- [7] R.B. Wiringa, V.G.J. Stoks, R. Schiavilla, Phys. Rev. C 51 (1995) 38.
- [8] R. Machleidt, F. Sammarruca, Y. Song, Phys. Rev. C 53 (1996) 1483.
- [9] G. Hoehler, et al., Nucl. Phys. B 114 (1976) 505.
- [10] W. Glöckle, The Quantum-Mechanical Few-Body Problem, Springer-Verlag, Berlin, 1983.
- [11] W. Glöckle, T.S.H. Lee, F. Coester, Phys. Rev. C 33 (1986) 709.
- [12] A.S. Raskin, T.W. Donnelly, Ann. Phys. 191 (1989) 78.
- [13] D. Rohe, et al., Phys. Rev. Lett. 83 (1999) 4257.
- [14] K. Aulenbacher, et al., Nucl. Instrum. Methods A 391 (1997) 498.
- [15] K.I. Blomqvist, et al., Nucl. Instrum. Methods A 403 (1998) 263.
- [16] R. Surkau, et al., Nucl. Instrum. Methods A 384 (1997) 444.
- [17] A. Amroun, et al., Nucl. Phys. A 579 (1994) 596.
- [18] E. Wilms, et al., Nucl. Instrum. Methods A 401 (1997) 491.